UC Berkeley
UC Berkeley Previously Published Works

Title

Mechanism of Photoredox-Initiated C–C and C–N Bond Formation by Arylation of IPrAu(I)–CF3 and IPrAu(I)–Succinimide

Permalink

Journal

ISSN

Authors

Kim, Suhong
Toste, F Dean

Publication Date

2019-03-13

DOI

Peer reviewed

Mechanism of Photoredox-Initiated C–C and C–N Bond Formation by Arylation of IPrAu(I)–CF$_3$ and IPrAu(I)–Succinimide

Suhong Kim and **F. Dean Toste**[*]

Department of Chemistry, University of California, Berkeley, California 94720, United States

Abstract

Herein, we report on the photoredox-initiated gold-mediated C(sp^2)–CF$_3$ and C(sp^2)–N coupling reactions. By adopting gold as a platform for probing metallaphotoredox catalysis, we demonstrate that cationic gold(III) complexes are the key intermediates of the C–C and C–N coupling reactions. The high-valent gold(III) intermediates are accessed by virtue of photoredox catalysis through a radical chain process. In addition, the bond-forming step of the coupling reactions is the reductive elimination from cationic gold(III) intermediates, which is supported by isolation and crystallographic characterization of key Au(III) intermediates.

Graphical Abstract
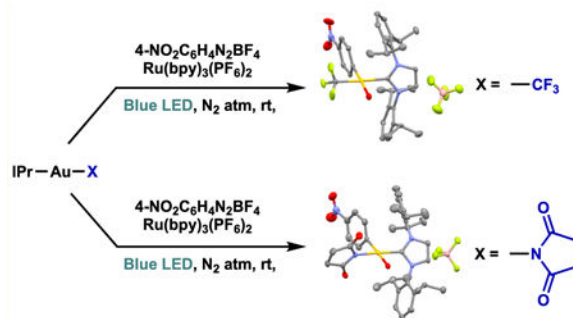
■ INTRODUCTION

The merger of photoredox catalysis and transition metal catalysis has enabled novel modes of reactivity via organic radical intermediates and odd-electron transition metal intermediates.[1] While this synergistic combination has been incredibly successful in upgrading the arsenal of synthetic chemists,[2] current mechanistic understanding of key

[*]**Corresponding Author**: fdtoste@berkeley.edu.

bond-forming events remains limited. Transition metal catalysts and intermediates are subject to various visible light-induced reactions such as charge-transfer, electron-transfer, and energy-transfer that can complicate mechanistic analysis. For example, in the case of nickel/photoredox dual catalysis, the Doyle group proposed photolysis of aryl nickel(III) chloride intermediates and metal to ligand charge transfer (MLCT) of aryl nickel(II) halide intermediates as elementary steps.[3] These light-induced processes, combined with the potential for odd electron intermediates and the instability of high-valent transition metal complexes, can make the details of the bond-forming step often difficult to ascertain.

A number of possibilities exist for the mechanism of bond formation in combined photoredox-transition metal catalysis, including a traditional reductive elimination,[4] radical substitution,[5,6] or radical recombination (Scheme 1A).[7] For example, copper/photoredox dual catalysis has been used by the MacMillan group to facilitate the formation of C−N bonds. These reactions are proposed to proceed via reductive elimination from a copper(III) intermediate (Scheme 1B).[8] On the other hand, under the photoinduced Ullmann C−N coupling conditions reported by the Fu and Peters groups, the prevailing explanation for C−N bond-forming step is radical substitution reaction between copper(II) intermediates and carbon-centered radical intermediates (Scheme 1C).[9] In this latter case, EPR and radical clock experiments are consistent with copper(II) and aryl radical species; however, the formation of a copper(III) intermediate has yet to be directly observed or excluded from a light-induced transformation. These mechanistic considerations are challenging to address due to the short lifetimes of radical and postulated high-valent copper(III) intermediates, especially under metallaphotoredox catalysis conditions.

Light-promoted reactivity, particularly involving aryl diazonium salts,[10,11] has also recently been leveraged to enable gold-catalyzed transformations. Moreover, gold complexes have been employed as photoredox catalysts for transformations of alkyl halides that are similar to the aforementioned copper-catalyzed processes.[12] Theoretical calculations support a mechanism involving the generation of gold(III) intermediates;[13] however, as is the case with copper catalysis, isolation of a photoredox-generated coordinatively unsaturated gold(III) complex capable of bond-formation through reductive elimination[14] has proven challenging.[15]

Recent studies from our group demonstrated that reductive elimination of trifluoromethylgold(III) complexes is a viable strategy to forge C−CF$_3$ bonds;[16] therefore, we hypothesized that diamagnetic gold(III) complexes generated from a photoredox-mediated oxidative addition might be isolated and characterized. Moreover, in direct analogy to Kochi's seminal mechanistic studies on the use of gold(I/III) as a mechanistic probe for gaining insight into carbon−carbon bond formation from copper(III), isolation of the gold(III) complex may provide insight into the copper(III) complexes proposed as intermediates in metallaphotoredox cross-coupling catalysis.[17] Trapping of these intermediates, presumably as less reactive and detectable d8-square planar complexes, would also allow for examination of the viability of the bond-forming event. Ultimately, on the basis of our understanding of the intermediates, we hoped to elucidate the bond-forming step of gold-mediated photoreodox catalysis and, eventually, to provide mechanistic insight to related heretofore uncharacterized metallaphotoredox processes.

Finally, we realized if mechanistic evidence supported the reductive elimination as the bond-forming step, we could also take advantage of these findings to examine other unprecedented reductive elimination reaction at gold(III). For example, we were especially intrigued by $C(sp^2)$–N coupling reactions due the dearth of examples of C–N reductive elimination from gold(III) complexes and the ambiguity over the copper(III) intermediates in the copper-catalyzed $C(sp^2)$– amide coupling reactions. Although copper(III)-mediated $C(sp^2)$–N reductive elimination is supported by stoichiometric reactions of well-defined aryl –copper(III) complexes,[18] and the formation of free aryl radical intermediates during the copper-catalyzed $C(sp^2)$–amide coupling reaction is not plausible,[19] the formation of copper(III) intermediates during the catalytic reactions remains inconclusive.[20] In this study, we provide mechanistic support for the formation of high-valent gold intermediates during photoredox-initiated gold-mediated $C(sp^2)$–CF_3 and $C(sp^2)$–N coupling reactions.

■ RESULTS AND DISCUSSION

We decided to investigate the reaction mechanism of photoredox-initiated gold-mediated $C(sp^2)$–CF_3 coupling reaction as a consequence of the following consideration. All three proposed bond-forming scenarios (Scheme 1A) are plausible with a trifluoromethyl group, and, as a result, the accessible reaction mechanism is not biased.[21] Also, if transition metal trifluoromethyl complexes are involved, undesired side reactions such as hydrogen atom transfer and β-hydride elimination from the resulting trifluoromethylgold(III) intermediates could be largely ignored.

With this in mind, we sought conditions for the photoredox-induced coupling of trifluoromethylgold(I) complex **1** with 4-nitrophenyl diazonium tetrafluoroborate. The desired $C(sp^2)$–CF_3 coupling product was obtained in 60% yield using nitromethane as a solvent, 1 equiv of **1**, and 1.5 equiv of 4-nitrophenyl diazonium tetrafluoroborate (Table 1, entry 1). Control experiments support that both the ruthenium complex and light are required for the reaction to proceed (Table 1, entries 2 and 3). The analogous iodonium electrophile was not as efficient as the diazonium salt (Table 1, entry 4), and significantly less of the desired product was formed when the $Ru(bpy)_3(PF_6)_2$ was replaced by other photoredox catalysts (Table 1, entries 5–9). The exclusion of air and water from the reaction media was critical for efficient reaction (Table 1, entries 10 and 11).

When water was present in the reaction mixture, instead of the desired product, another CF_3-containing species was observed by 19F NMR (55% yield in Table 1, entry 11). We postulated that this trifluoromethyl-containing species might be the four-coordinate gold(III) intermediate with one of the coordination sites occupied by water, thereby inhibiting reductive elimination (Scheme 2). This hypothesis led us to evaluate other coordinating aprotic polar solvents. In the event, replacing nitromethane with acetonitrile provided the analogous CF_3-containing gold(III) acetonitrile complex. In this case, other CF_3-containing species such as the starting gold(I) complex, the coupling product, and any other side products were not detected using ^{19}F NMR (Figure 1).

This new species, **4**, was analyzed by HRMS, ^{13}C NMR, and ^1H NOESY (see the Supporting Information). Two new quartets in the ^{13}C NMR spectrum with $^3J_{C-F}$ values of

25 and Hz, respectively, support that the IPr, CF_3, and 4-nitrophenyl are all bound on the same gold atom but in a different stereochemical relationship. [1]H NOE between IPr and 4-nitrophenyl supports that they are *cis* to each other, and therefore we predicted the CF_3 group was *trans* to the IPr ligand. After the acetonitrile-bound gold(III) intermediate was characterized by NMR studies, the gold(III) aquo complex was crystallized as the tetrafluoroborate salt. The structure was analyzed by single-crystal X-ray diffraction and further supported the aforementioned spectroscopic characterizations (Figure 2).[14]

On the basis of this evidence for the formation of a gold(III) complex as an intermediate, we sought to unravel the mechanism of photoredox-promoted oxidative addition. To gain a deeper insight into the role of the visible light in this transformation, the emission spectrum of the light source, Kessil H150, was compared to the absorption spectra of all chemical compounds in the reaction mixture. Although there are examples in which gold complexes initiate radical reactions as photosensitizers,[12] we observed that the radiated visible light was exclusively absorbed by the ruthenium photoredox catalysts in our system (Figure 3). This conclusion is further supported by the previously performed control experiment (Table 1, entry 2).

To explore the elementary step following the excitation of the photoredox catalyst, a photoluminescence quenching experiment was performed. The Stern–Volmer relationship supports the hypothesis that only the aryldiazonium salt reacts with the excited photoredox catalyst (Figure 4, see the Supporting Information). An electron-transfer process is supported by the evolution of nitrogen gas upon radiation of visible light in the absence of gold complexes.[22]

The generation of odd-electron intermediates from photoluminescence quenching suggests that oxidative addition could proceed through a gold(II) intermediate. Two distinct gold(II) intermediates were considered: a neutral or a cationic gold(II) species (Figure 5). The cationic pathway would presumably result from oxidation of the gold(I) complexes by the photoredox catalysts. To clarify whether the Ru(III) intermediate is capable of oxidizing IPrAuCF$_3$, the cyclic voltammogram of both Ru(bpy)$_3$(PF$_6$)$_2$ and IPrAuCF$_3$ was measured and showed that the redox potential of Ru(II)/ Ru(III) is not adequate to oxidize IPrAuCF$_3$ to the corresponding cationic gold(II) intermediate (Figure 5, see the Supporting Information). As a result, we envision that the free aryl radical reacts directly with **1** to generate a neutral (trifluoromethyl)arylgold(II) intermediate.

With the implication of the neutral gold(II) intermediate and the direct observation of a trifluoromethylgold(III) species, we sought to ascertain the oxidant responsible for the single electron oxidation from the gold(II) to gold(III). To this end, the quantum yield of oxidative addition was mearsured.[23] By radiating 3.3 mol % of photons over 20 min in a fluorometer at room temperature, the nitromethane-ligated trifluoromethylgold(III) complex was observed in 22% yield; but, the reductive elimination product was not detected (Figure 6, see the Supporting Information). The quantum yield of 6.6 implies that the oxidative addition involves a chain process, wherein the gold(II) intermediate is mainly oxidized by aryldiazonium. Furthermore, in sharp contrast to the CH$_3$CN and H$_2$O-bound gold(III) complexes, the CH$_3$NO$_2$-bound gold(III) complex readily underwent quantitative reductive

elimination upon heating up to 40 °C (Figure 6). This observation suggests that the activation barrier of reductive elimination might be overcome by heat from the light source.[24]

During quantum yield measurements, we also uncovered a chain terminating event. The presence of unreacted $IPrAuCF_3$ and 4-nitrophenyl diazonium salts indicates that the chain propagation is interrupted. According to a previous report on gold(II) intermediates,[8] we proposed the release of trifluoromethyl radical from the gold(II) intermediate as the chain terminating event (Figure 6, path K). Additionally, given that this process competes with oxidation of the gold(II) intermediate, the electronic properties of aryldiazonium are expected to influence the yield of the reaction. As we hypothesized, a decrease in product yield was observed as the σ_{para} of substituents inverts from positive values (Table 2, entries 1–6) to negative values (Table 2, entries 8–10). Moreover, to support the release of trifluoromethyl radical, we attempted to intercept the trifluoromethyl radical with radical traps. Addition of 70 equiv of benzene to the optimized reaction condition produced trifluoromethylbenzene as a major product (Scheme 3, see the Supporting Information).[25]

Having gained evidence for the stepwise formation of a gold(III) intermediate as relevant to the C–C bond formation in the photoredox-promoted gold-mediated $C(sp^2)$–CF_3 coupling reaction, we sought to apply these mechanistic insights to examine the possibility that a similar pathway is involved in previously unknown photoredox driven $C(sp^2)$–N bond formation.

In the event, the product (**6**) of the photoredox-initiated gold-mediated $C(sp^2)$–N coupling reaction was obtained in 68% yield from gold(I)–succinimide (**5**) by only slight modification of the reaction conditions previously employed for trifluoromethylation (Scheme 4). It is notable that other gold–amides did not undergo the C–N bond-forming reaction with the same efficiency; rather, competitive protodeauration (formation of an N–H bond) was observed. Notably, the relative stability of the *N*-centered radical species that would be generated by Au–N bond scission appears to be irrelevant to the efficiency of the gold-mediated $C(sp^2)$–N coupling reactions. On the basis of additional experiments (see the Supporting Information), we propose that the nature of the amide ligand is important for suppressing uncatalyzed reactions of the gold(I)–amide, such as direct oxidation by the photoredox catalyst or reaction with electrophilic diazonium salt. This hypothesis is consistent with our previous observations that gold(I)–amides show increased nucleophilicity.[26]

To further explore the possibility that high-valent gold(III) intermediates are involved in the $C(sp^2)$–N coupling reaction, experiments to intercept the potential gold(III) imide intermediate were untaken (Scheme 5). These experiments resulted in the successful isolation and characterization of a gold(III) aquo succinimide complex (Figure 7). The isolation of this gold(III) species from a photoredox-initiated process is consistent with the hypothesis that the photoredox-promoted gold-mediated $C(sp^2)$–succinimide coupling reaction proceeds by a mechanism closely related to that established for the photoredox-initiated gold-mediated $C(sp^2)$–CF_3 coupling reaction: oxidative addition followed by gold(III)-centered $C(sp^2)$–N reductive elimination.

■ CONCLUSION

In summary, the unique characteristics of gold have simplified the mechanistic understanding of metallaphotoredox-mediated trifluoromethylation. This reaction was initiated by visible light in the presence of a photoredox catalyst. Evidence was gained in support of a mechanistic scenario involving addition of the aryl radical to trifluoromethylgold(I) complex to generate a gold(II) species that undergoes a single electron oxidation to access the gold(III) intermediate. This oxidation likely occurs by reaction of the gold(II) species with the aryldiazonium salt, thereby generating an aryl radical. This chain mechanism is consistent with the measured quantum yield (6.6) for the process. After radical chain oxidative addition, the gold(III) intermediate, which was isolable in coordinating solvents, is converted to the desired product via reductive elimination (Figure 8). We propose that the reductive elimination, which regenerates gold(I), is the bond-forming step of photoredox-initiated gold-mediated $C(sp^2)$–CF_3 and $C(sp^2)$–N coupling reactions. To the best of our knowledge, the analogous copper(III) intermediates in copper/photoredox dual catalytic trifluoromethylation and amination reactions have not been isolated or characterized. Thus, the use of gold, as another member of group 11, may provide useful insight into the mechanism of these metallaphotoredox-catalyzed transformations.

Supplementary Material

Refer to Web version on PubMed Central for supplementary material.

ACKNOWLEDGMENTS

REFERENCES

(1). (a)For reviews of metallaphotoredox catalysis, see: Twilton J; Le C; Zhang P; Shaw MH; Evans RW; MacMillan DWC The merger of transition metal and photocatalysis. Nat. Rev. Chem 2017, 1, 52.(b)Levin MD; Kim S; Toste FD Photoredox Catalysis Unlocks Single-Electron Elementary Steps in Transition Metal Catalyzed Cross-Coupling. ACS Cent. Sci 2016, 2, 293–301. [PubMed: 27280163] (c)Skubi KL; Blum TR; Yoon TP Dual Catalysis Strategies in Photochemical Synthesis. Chem. Rev 2016, 116, 10035–10074. [PubMed: 27109441] (d)Hopkinson MN; Sahoo B; Li J-L; Glorius F Dual Catalysis Sees the Light: Combining Photoredox with Organo-, Acid, and Transition-Metal Catalysis. Chem. - Eur. J 2014, 20, 3874–3886. [PubMed: 24596102] (e)Prier CK; Rankic DA; MacMillan DWC Visible Light Photoredox Catalysis with Transition Metal Complexes: Applications in Organic Synthesis. Chem. Rev 2013, 113, 5322–5363. [PubMed: 23509883]

(2). (a)For seminal reports, see: Tellis JC; Primer DN; Molander GA Single-electron transmetalation in organoboron cross-coupling by photoredox/nickel dual catalysis. Science 2014, 345, 433–436. [PubMed: 24903560] (b)Zuo Z; Ahneman DT; Chu L; Terrett JA; Doyle AG; MacMillan DWC Merging photoredox with nickel catalysis: Coupling of a-carboxyl sp^3-carbons with aryl halides. Science 2014, 345, 437–440. [PubMed: 24903563] (c)Tasker SZ; Jamison TF Highly Regioselective Indoline Synthesis under Nickel/Photoredox Dual Catalysis. J. Am. Chem. Soc

2015, 137, 9531–9534. [PubMed: 26196355] (d)Terrett JA; Cuthbertson JD; Shurtleff VW; MacMillan DWC Switching on elusive organometallic mechanisms with photoredox catalysis. Nature 2015, 524, 330–334. [PubMed: 26266976] (e)Kalyani D; McMurtrey KB; Neufeldt SR; Sanford MS Room-Temperature C–H Arylation: Merger of Pd-Catalyzed C–H Functionalization and Visible-Light Photocatalysis. J. Am. Chem. Soc 2011, 133, 18566–18569. [PubMed: 22047138] (f)Ye Y; Sanford MS Merging Visible-Light Photocatalysis and Transition-Metal Catalysis in the Copper-Catalyzed Trifluoromethylation of Boronic Acids with CF$_3$I. J. Am. Chem. Soc 2012, 134, 9034–9037. [PubMed: 22624669]

(3). (a) Shields BJ; Doyle AG Direct C(sp^3)–H Cross Coupling Enabled by Catalytic Generation of Chlorine Radicals. J. Am. Chem. Soc 2016, 138, 12719–12722. [PubMed: 27653738] (b)Shields BJ; Kudisch B; Scholes GD; Doyle AG Long-Lived Charge-Transfer States of Nickel(II) Aryl Halide Complexes Facilitate Bimolecular Photoinduced Electron Transfer. J. Am. Chem. Soc 2018, 140, 3035–3039 [PubMed: 29400956] (c)See also:. Sun R; Qin Y; Ruccolo S; Schnedermann C; Costentin C; Nocera DG Elucidation of a Redox-Mediated Reaction Cycle for Nickel-Catalyzed Cross Coupling. J. Am. Chem. Soc 2019, 141, 89–93.

(4). Hartwig JF Carbon–Heteroatom Bond-Forming Reductive Eliminations of Amines, Ethers, and Sulfides. Acc. Chem. Res 1998, 31, 852–860.

(5). (a)For perfluorinated alkyl radicals, see: Bravo A; Bjørsvik HR; Fontana F; Liguori L; Mele A; Minisci F New Methods of Free-Radical Perfluoroalkylation of Aromatics and Alkenes. Absolute Rate Constants and Partial Rate Factors for the Homolytic Aromatic Substitution by n-Perfluorobutyl Radical. J. Org. Chem 1997, 62, 7128–7136. [PubMed: 11671816] (b)Studer AA "Renaissance" in Radical Trifluoromethylation. Angew. Chem., Int. Ed 2012, 51, 8950–8958.

(6). (a)For N-centered radicals, see: Kärkäs MD Photochemical Generation of Nitrogen-Centered Amidyl, Hydrazonyl, and Imidyl Radicals: Methodology Developments and Catalytic Applications. ACS Catal 2017, 7, 4999–5022.(b)Zard SZ Recent progress in the generation and use of nitrogen-centred radicals. Chem. Soc. Rev 2008, 37, 1603–1618. [PubMed: 18648685] (c)Xiong T; Zhang Q New amination strategies based on nitrogen-centered radical chemistry. Chem. Soc. Rev 2016, 45, 3069–3087. [PubMed: 27116936]

(7). In the recent example of copper/photoredox dual catalytic aryl trifluoromethylation, both CF$_3$ radical and carbon(sp^2)-centered radicals were proposed as viable intermediates. Le C; Chen TQ; Liang T; Zhang P; MacMillan DWC A radical approach to the copper oxidative addition problem: Trifluoromethylation of bromoarenes. Science 2018, 360, 1010–1014. [PubMed: 29853683]

(8). Liang Y; Zhang X; MacMillan DWC Decarboxylative sp^3 C–N coupling via dual copper and photoredox catalysis. Nature 2018, 559, 83–88. [PubMed: 29925943]

(9). (a) Creutz SE; Lotito KJ; Fu GC; Peters JC Photoinduced Ullmann C–N Coupling: Demonstrating the Viability of a Radical Pathway. Science 2012, 338, 647–651. [PubMed: 23118186] (b)Bissember AC; Lundgren RJ; Creutz SE; Peters JC; Fu GC Transition-Metal-Catalyzed Alkylations of Amines with Alkyl Halides: Photo-induced, Copper-Catalyzed Couplings of Carbazoles. Angew. Chem., Int. Ed 2013, 52, 5129–5133.(c)Ziegler DT; Choi J; Muñoz-Molina JM; Bissember AC; Peters JC; Fu GC A Versatile Approach to Ullmann C–N Couplings at Room Temperature: New Families of Nucleophiles and Electrophiles for Photoinduced, Copper-Catalyzed Processes. J. Am. Chem. Soc 2013, 135, 13107– 13112. [PubMed: 23968565] (d)Do H; Bachman S; Bissember AC; Peters JC; Fu GC Photoinduced, Copper-Catalyzed Alkylation of Amides with Unactivated Secondary Alkyl Halides at Room Temperature. J. Am. Chem. Soc 2014, 136, 2162–2167. [PubMed: 24446666] (e)Kainz QM; Matier CD; Bartoszewicz A; Zultanski SL; Peters JC; Fu GC Asymmetric copper-catalyzed C-N cross-couplings induced by visible light. Science 2016, 351, 681–684. [PubMed: 26912852]

(10). (a)For examples involving the functionalization of π-bonds, see: Sahoo B; Hopkinson MN; Glorius F Combining Gold and Photoredox Catalysis: Visible Light Mediated Oxy and Amino-arylation of Alkenes. J. Am. Chem. Soc 2013, 136, 7777–7782.(b)Shu X-z.; Zhang M; He Y; Frei H; Toste FD J. Am. Chem. Soc 2014, 136, 5844–5847. [PubMed: 24730447] (c)Hopkinson MN; Sahoo B; Glorius F Dual Photoredox and Gold Catalysis: Intermolecular Multicomponent Oxyarylation of Alkenes. Adv. Synth. Catal 2014, 356, 2794–2800.(d)Huang L; Rudolph M; Rominger F; Hashmi ASK Photosensitizer-Free Visible-Light-Mediated Gold-Catalyzed 1,2-Difunctionalization of Alkynes. Angew. Chem., Int. Ed 2016, 55, 4808–4813.(e)Patil DV; Yun H;

Shin S Catalytic Cross-Coupling of Vinyl Golds with Diazonium Salts under Photoredox and Thermal Conditions. Adv. Synth. Catal 2015, 357, 2622–2628.(f)Um J; Yun H; Shin S Cross-Coupling of Meyer-Schuster Intermediates under Dual Gold-Photoredox Catalysis. Org. Lett 2016, 18, 484–487. [PubMed: 26761155] (g)Alcaide B; Almendros P; Busto E; Luna A Domino Meyer-Schuster/Arylation Reaction of Alkynols or Alknynl Hydroperoxides with Diazonium Salts Promoted by Visible Light under Dual Gold and Ruthenium Catalysis. Adv. Synth. Catal 2016, 358, 1526–1533.(h)Xia Z; Khaled O; Mouries-Mansuy V; Ollivier C; Fensterbank L Dual Photoredox/Gold Catalysis Arylative Cyclization of o-Alkynylphenols with Aryldiazonium Salts: A Flexible Synthesis of Benzofurans. J. Org. Chem 2016, 81, 7182. [PubMed: 27362460] (i)Bansode AH; Shaikh SR; Gonnade RG; Patil NT Intramolecular ipso-arylative cyclization or aryl-alkynoates and N-arylpropiolamides with aryldiazonium salts through merged gold/ visible photoredox catalysis. Chem. Commun 2017, 53, 9081–9084.(j)Alciade B; Almendros P; Aparicio B; La aro-Milla C; Luna A; Faza ON Gold-Photoredox-Cocatalyzed Tandem Oxycyclizaion /Coupling Sequence of Allenols and Diazonium Salts with Visible Light Mediation. Adv. Synth. Catal 2017, 359, 2789–2800.(k)Deng J-R; Chan W-C; Lai NC-H; Yang B; Tsang C-S; Ko BC-B; Chan SL-F; Wong MK Photosensitizer-free visible light mediated gold-catalysed cis-difunctionalization of silyl-substituted alkynes. Chem. Sci 2017, 8, 7537–7544. [PubMed: 29163908]

(11). (a)For examples of cross-coupling reactions, see: He Y; Wu H; Toste FD A dual catalytic strategy for carbon-phosphorus cross-coupling via gold and photoredox catalysis. Chem. Sci 2015, 6, 1194– 1198. [PubMed: 25685313] (b)Cai R; Lu M; Aguilera EY; Xi X; Akhemdov NG; Petersen JL; Chen H; Shi X Ligand-Assisted Gold-Catalyzed Cross-Coupling with Aryldiazonium Salts: Redox Gold Catalysis without and External Oxidant. Angew. Chem. Int. Ed 2015, 54, 8772–8776.(c)Tlahuext-Aca A; Hopkinson MN; Sahoo B; Glorius F Dual gold/phtoredox-catalyzed C(sp)-H arylation of terminal alkynes with diazonium salts. Chem. Sci 2016, 7, 89–93. [PubMed: 29861968] (d)Kim S; Rojas-Martin J; Toste FD Visible light-mediated gold-catalyzed carbon(sp^2)-carbon(sp) cross-coupling. Chem. Sci 2016, 7, 85–88. [PubMed: 29861967] (e)Gauchot V; Lee A-L Dual gold photoredox C(sp^2)-C(sp^2) cross coupling – development and mechanistic studies. Chem. Commun 2016, 52, 10163–10166.(f)Cornilleau T; Hermange P; Fouquet E Gold-catalyzed cross-coupling between aryldiazonium salts and arylboronic acids: probing the usefulness of conditions. Chem. Commun 2016, 52, 10040–10043.(g)Witzel S; Xie J; Rudolph M; Hashmi ASK Photosensitizer-Free, Gold-Catalyzed Cross-Coupling of Boronic Acids and Diazonium Salts Enabled by Visible Light. Adv. Synth. Catal 2017, 359, 1522–1528. (h)Sauerm C; Liu Y; De Nisi A; Protti S; Fagnoni M; Bandini M Photocatalyst-free, Visible Light Driven, Gold Promoted Suzuki Synthesis of (Hetero)biaryls. ChemCatChem 2017, 9, 4456–4459. (i)Xie J; Sekine K; Witzel S; Krämer P; Rudolph M; Rominger F; Hashmi ASK Light-Induced Gold-Catalyzed Hiyama Arylation: A Coupling Access to Biarylboronates. Angew. Chem. Int. Ed 2018, 57, 16648–16653.(j)Witzel S; Sekine K; Rudolph M; Hashmi ASK New transmetalation reagents for the gold-catalyzed visible light-enabled C(sp or sp^2)-C(sp^2) cross-coupling wth aryldiazonium salts in the absence of photosensitizer. Chem. Commun 2018, 54, 13802–13804.

(12). (a)For gold complex as photosensitizers for reactions of alkylhalides, see: Revol G; McCallum T; Morin M; Gagosz F; Barriault L Angew. Chem., Int. Ed 2013, 52, 13342–13345.(b)McCallum T; Slavko E; Morin M; Barriault L Light-Mediated Deoxygenation of Alcohols with a Dimeric Gold Catalyst. Eur. J. Org. Chem 2015, 2015, 81–85.(c)Kaldas SJ; Cannillo A; McCallum T; Barriault L Indole Funcationalization via Photoredox Gold Catalysis. Org. Lett 2015, 17, 2864–2866. [PubMed: 25997468] (d)Xie J; Zhang T; Chen F; Mehrkens N; Rominger F; Rudolph M; Hashmi ASK Gold-Catalyzed Highly Selective Photoredox C(sp2)-H Difluoroalkylation and Perfluoroalkylation of Hydrazones. Angew. Chem., Int. Ed 2016, 55, 2934–2938.(e)Tran H; McCallum T; Morin M; Barriault L Homocoupling of Iodoarenes and Bromoalkanes Using Photoredox Gold Catalysis. Org. Lett 2016, 18, 4308–4311. [PubMed: 27522864] (f)Cannillo A; Schwantje TR; Bégin M; Barabé F; Barriaultm L Gold-Catalyzed Photoredox C(sp2) Cyclization: Formal Synthesis of (±)-Triptolide. Org. Lett 2016, 18, 2592– 2595. [PubMed: 27177198] (g)McCallum T; Barriault L Direct alkylation of heteroarenes with unactivated bromoalkanes using photoredox gold catalysis. Chem. Sci 2016, 7, 4754–4758. [PubMed: 30155127] (h)Xie J; Li J Intramolecular Photocatalyzed Heck-like coupling of Unactivated Alkyl Bromides by a Dinuclear Gold Complex. Chem. - Eur. J 2016, 22, 12646–12650. [PubMed:

27348503] (i)Rohe S; McCallum T; Morris AG; Barriault L Transformations of Isonitriles with Bromoalkanes Using Photoredox Gold Catalysis. J. Org. Chem 2018, 83, 10015–10024 For reactions with amines, see:. [PubMed: 29979602] (j)Xie J; Shi S; Zhang T; Mehrkens N; Rudolph M; Hashmi ASK A Highly Efficient Gold-Catalyzed Photoredox α-C(sp3)–H Alkynylation of Tertiary Aliphatic Amines with Sunlight. Angew. Chem., Int. Ed 2015, 54, 6046–6050.(k)Xie J; Rudolph M; Rominger F; Hashmi ASK Photoredox-Controlled Mono- and Di-Multifluoroarylation of C(sp^3)-H Bonds with Aryl Fluorides. Angew. Chem., Int. Ed 2017, 56, 7266–7270.

(13). (a) Zhang Q; Zhang Z-Q; Fu Y; Yu H-Z Mechanism of the Visible Light Mediated Gold-Catalyzed Oxyarylation Reaction of Alkenes. ACS Catal 2016, 6, 798–808.(b)Bhattacharjee R; Datta A Understanding Thernal and Photochemical Aryl-Aryl Cross-Coupling by the Au^I/Au^{III} Redox Couple. Chem. - Eur. J 2016, 24, 13636–13464.(c)Liu Y; Yang Y; Zhu R; Liu C; Zhang D The Dual Role of Gold(I) Complexes in Photosensitizer-Free Visible-Light-Mediated Gold-Catalyzed 1,2-Difunctionalization of Alkynes: A DFT Study. Chem. - Eur. J 2018, 24, 14119–14126. [PubMed: 30052273]

(14). (a) Tlahuext-Aca A; Hopkinson MN; Daniliuc CG; Glorius F Oxidative Addition to Gold(I) by Photoredox Catalysis: Straightforward Access to Diverse (C,N)-Cyclometalated Gold(III) Complexes. Chem. - Eur. J 2016, 22, 11587–11592. [PubMed: 27338119] (b)Huang L; Rominger F; Rudolph M; Hashmi ASK A general access to organogold(III) complexes by oxidative addition of diazonium salts. Chem. Commun 2016, 52, 6435–6438.(c)Asomoza-Solis EO; Rojas-Ocampo J; Toscano RA; Porcel S Arenediazonium salts as electrophiles for the oxidative addition of gold(I). Chem. Commun 2016, 52, 7295–7298.

(15). Wolf WJ; Winston MS; Toste FD Exceptionally fast carbon-carbon bond reductive elimination from gold(III). Nat. Chem 2014, 6, 159–164. [PubMed: 24451593]

(16). (a) Winston MS; Wolf WJ; Toste FD Photoinitiated Oxidative Addition of CF$_3$I to Gold(I) and Facile Aryl-CF$_3$ Reductive Elimination. J. Am. Chem. Soc 2014, 136, 7777–7782. [PubMed: 24836526] (b)Winston MS; Wolf WJ; Toste FD Halide-Dependent Mechanisms of Reductive Elimination from Gold(III). J. Am. Chem. Soc 2015, 137, 7921–7928. [PubMed: 26065722] (c)Levin MD; Chen TQ; Neubig ME; Hong CM; Theulier CA; Kobylianskii IJ; Janabi M; O'Neil JP; Toste FD A catalytic fluoride-rebound mechanism for C(sp^3)-CF3 bond formation. Science 2017, 356, 1272–1276. [PubMed: 28642435]

(17). (a) Tamaki A; Kochi JK Catalytic mechanism involving oxidative addition in the coupling of alkylgold(I) with alkyl halides. J. Organomet. Chem 1972, 40, C81–C84.(b)Tamaki A; Magennis SA; Kochi JK Rearrangement and decomposition of trialkylgold(III) complexes. J. Am. Chem. Soc 1973, 95, 6487–6488.(c)Tamaki A; Magennis SA; Kochi JK Catalysis by gold. Alkyl isomerization, cis-trans rearrangement, and reductive elimination of alkylgold(III) complexes. J. Am. Chem. Soc 1974, 96, 6140–6148.(d)Komiya S; Kochi JK Electrophilic cleavage of organogold complexes with acids. The mechanism of the reductive elimination of dialkyl(aniono)-gold(III) species. J. Am. Chem. Soc 1976, 98, 7599–7607.(e)Komiya S; Albright TA; Hoffmann R; Kochi JK The stability of organogold compounds. Hydrolytic, thermal, and oxidative cleavages of dimethylaurate(I) and tetramethylaurate(III). J. Am. Chem. Soc 1977, 99, 8440–8447.

(18). (a) Huffman LM; Stahl SS Carbon–Nitrogen Bond Formation Involving Well-Defined Aryl –Copper(III) Complexes. J. Am. Chem. Soc 2008, 130, 9196–9197. [PubMed: 18582057] (b)King AE; Huffman L; Casitas A; Costas M; Ribas X; Stahl SS Copper-Catalyzed Aerobic Oxidative Functionalization of an Arene C–H Bond: Evidence for an Aryl-Copper(III) Intermediate. J. Am. Chem. Soc 2010, 132, 12068–12073. [PubMed: 20690595] (c)Casitas A; King AE; Parella T; Costas M; Stahl SS; Ribas X Direct observation of Cu^I/Cu^{III} redox steps relevant to Ullmann-type coupling reactions. Chem. Sci 2010, 1, 326–330.

(19). Tye JW; Weng Z; Johns AM; Incarvito CD; Hartwig JF Copper Complexes of Anionic Nitrogen Ligands in the Amidation and Imidation of Aryl Halides. J. Am. Chem. Soc 2008, 130, 9971–9983. [PubMed: 18597458]

(20). Strieter ER; Bhayana B; Buchwald SL Mechanistic Studies on the Copper-Catalyzed N-Arylation of Amides. J. Am. Chem. Soc 2009, 131, 78–88. [PubMed: 19072233]

(21). Rubio J-G; Vincente J Gold trifluoromethyl complexes. Dalton Trans 2015, 44, 19432–19442. [PubMed: 26169553]

(22). Cano-Yelo H; Deronzier A Photocatalysis of the Pschorr reaction by tris-(2,2′-bipyridyl)ruthenium(II) in the phenanthrene series. J. Chem. Soc., Perkin Trans. 2 1984, 2, 1093–1098.

(23). Cismesia MA; Yoon TP Characterizing chain processes in visible light photoredox catalysis. Chem. Sci 2015, 6, 5426–5434. [PubMed: 26668708]

(24). Both thermal and photochemical reductive eliminations from NHC–gold complexes are plausible. Ghidiu MJ; Pistner AJ; Yap GPA; Lutterman DA; Rosenthal J Thermal versus Photochemical Reductive Elimination of Aryl Chlorides from NHC–Gold Complexes. Organometallics 2013, 32, 5026–5029.

(25). Nagib DA; MacMillan DWC Trifluoromethylation of arenes and heteroarenes by means of photoredox catalysis. Nature 2011, 480, 224–228. [PubMed: 22158245]

(26). Because of the repulsive interaction with d^{10} gold(I) metal, gold-bound nitrogen ligands become more nucleophilic. Johnson MW; Shevick SL; Toste FD; Bergman RG Preparation and reactivity of terminal gold(I) amides and phosphides. Chem. Sci 2013, 4, 1023–1027.
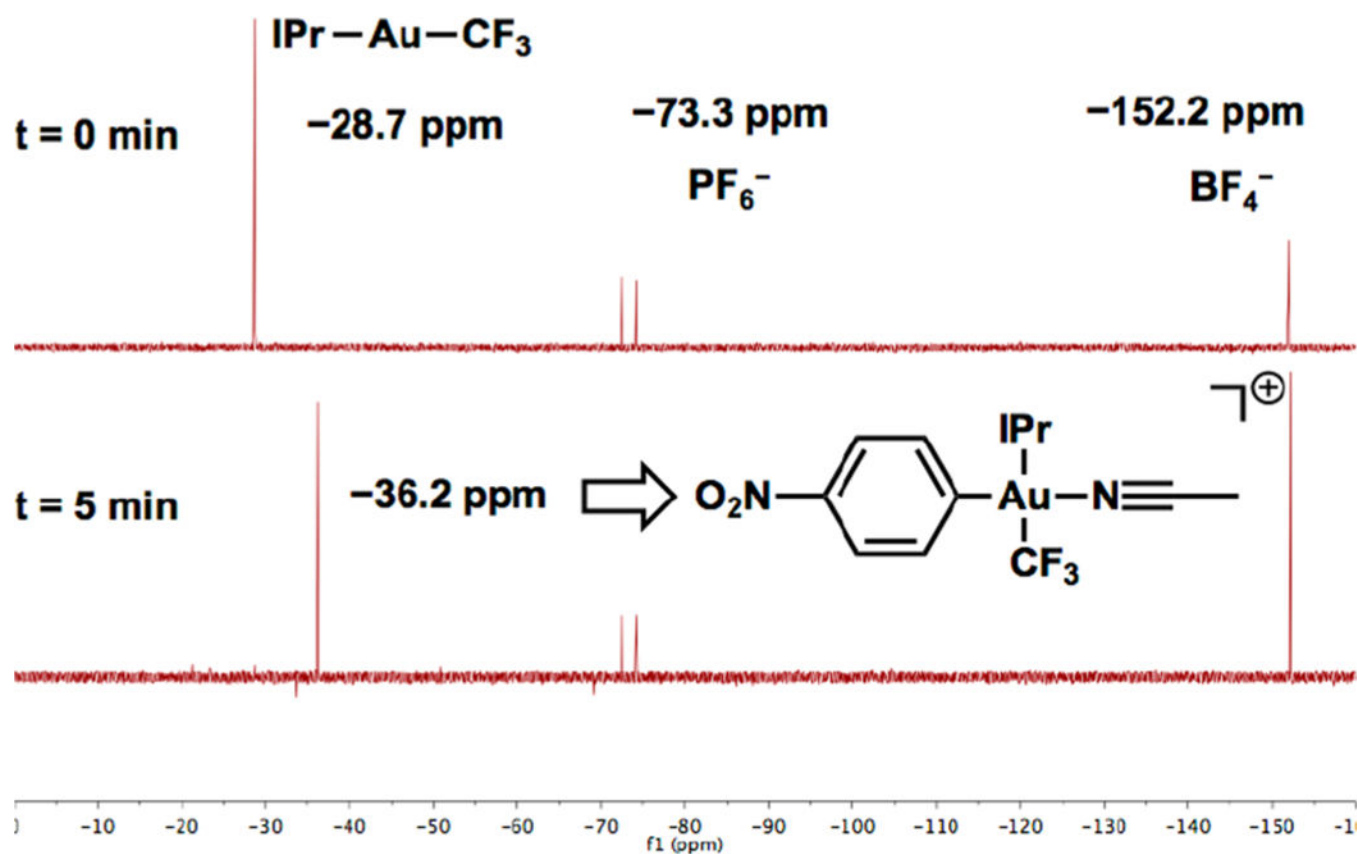
Figure 1.
^{19}F NMR spectra of gold-mediated $C(sp^2)–CF_3$ coupling reaction, solvent $= CH_3CN$.
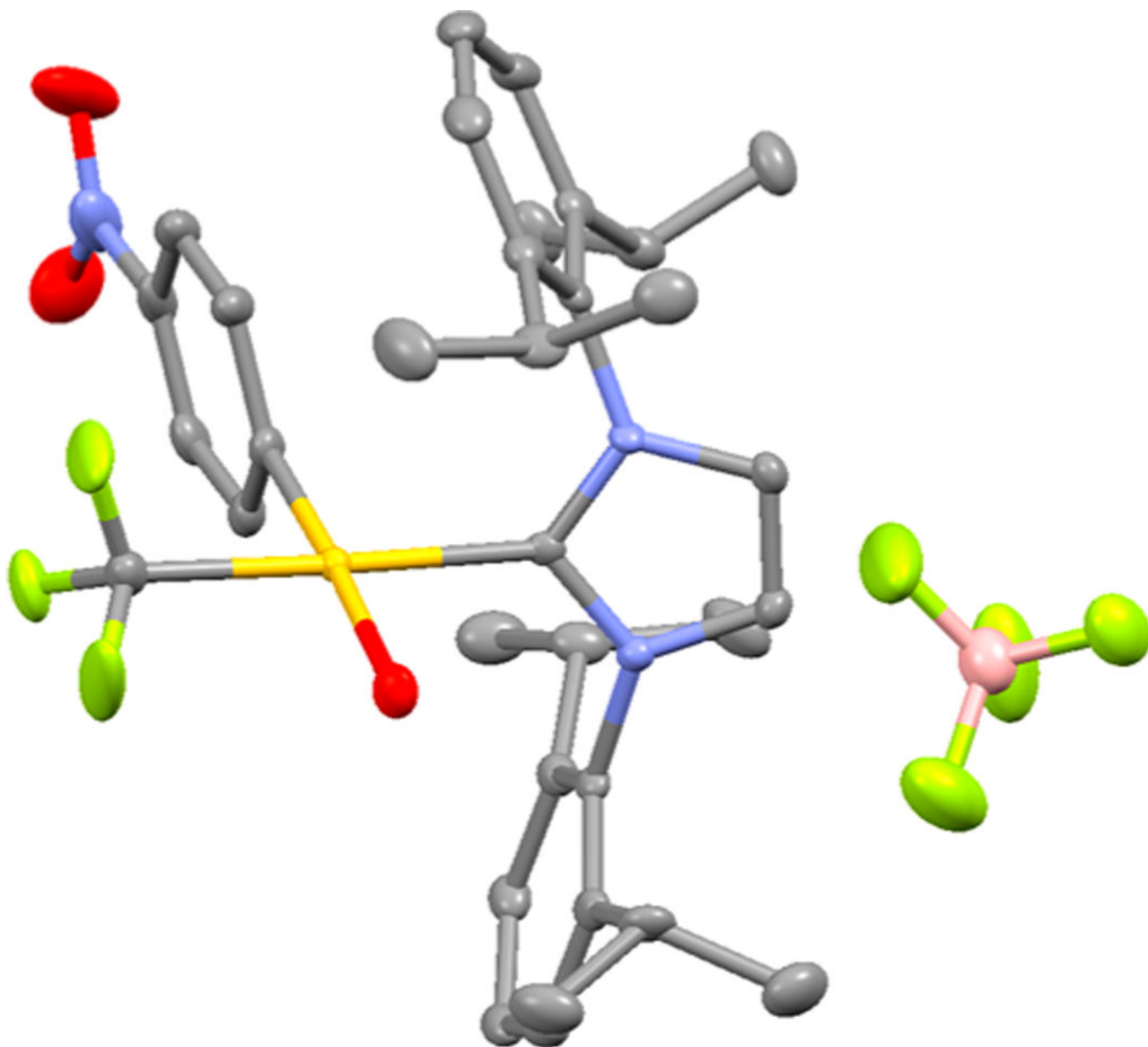
Figure 2.
Crystal structure of 3-BF$_4$. Thermal ellipsoid plot is drawn at 50% probability. Hydrogen atoms and solvents are omitted for clarity.
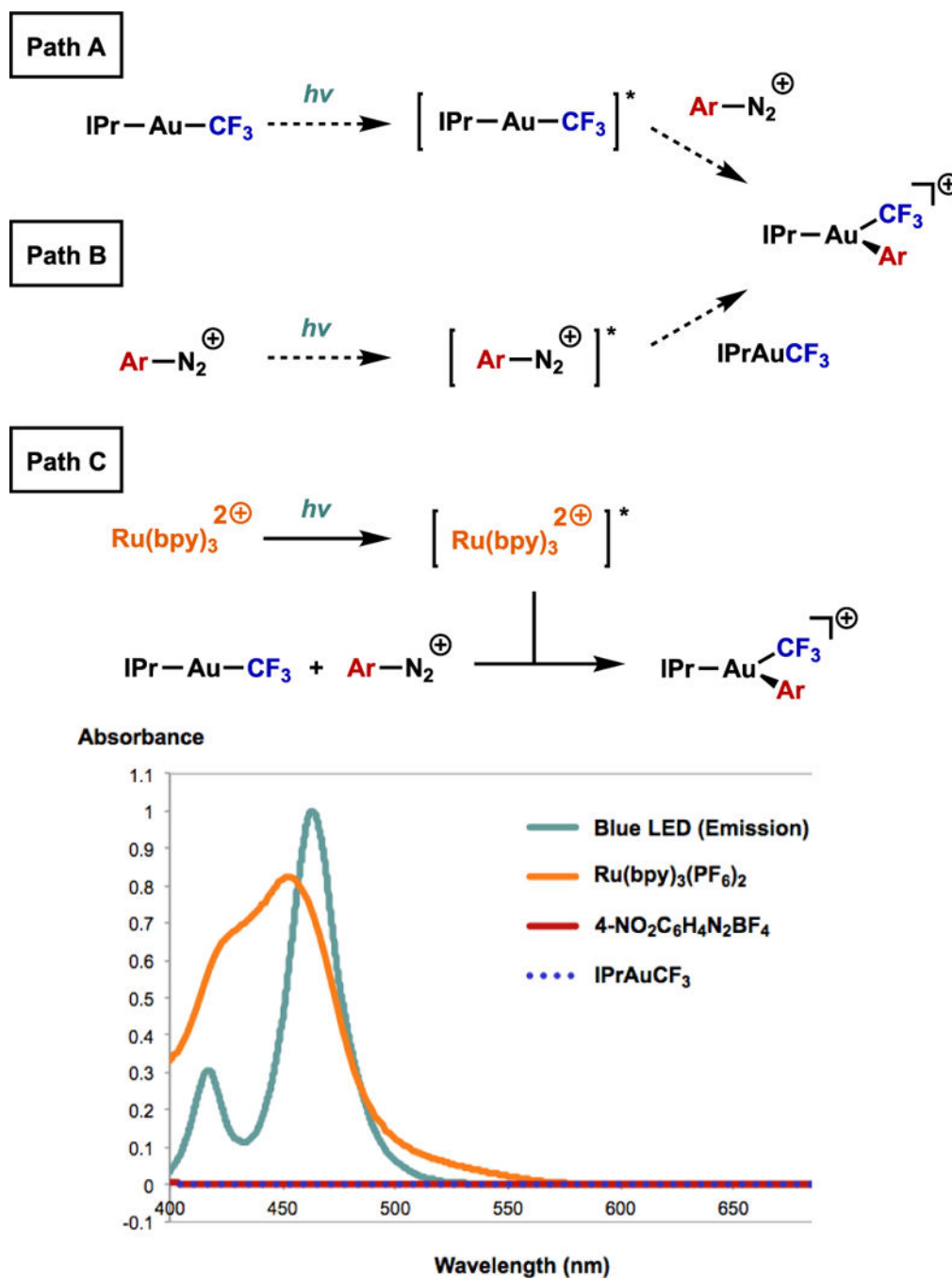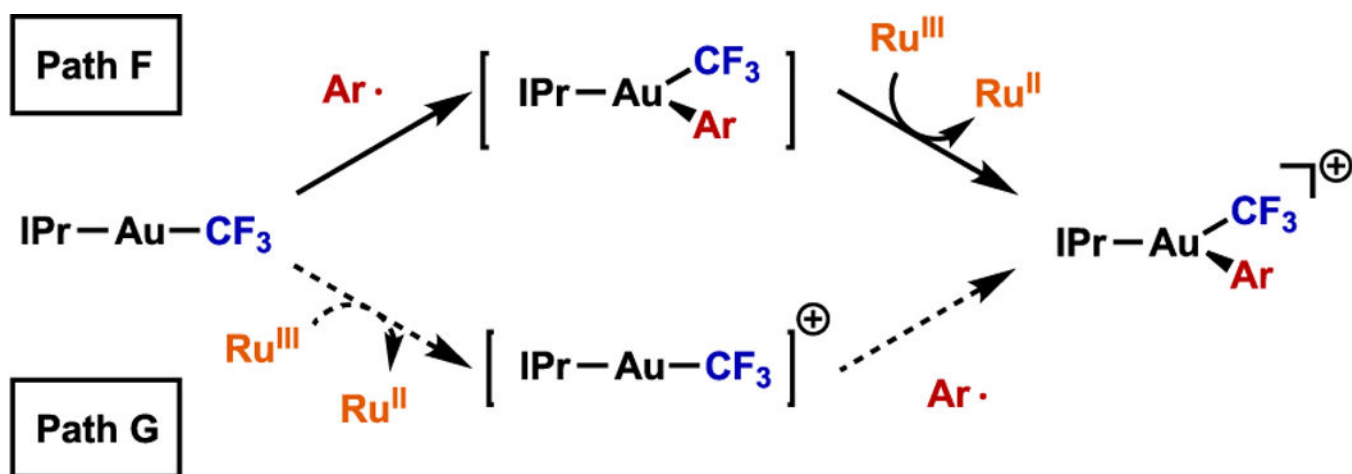
Figure 3.
(Top) Three possible modes of sensitization with visible light. Paths A and B were ruled out.
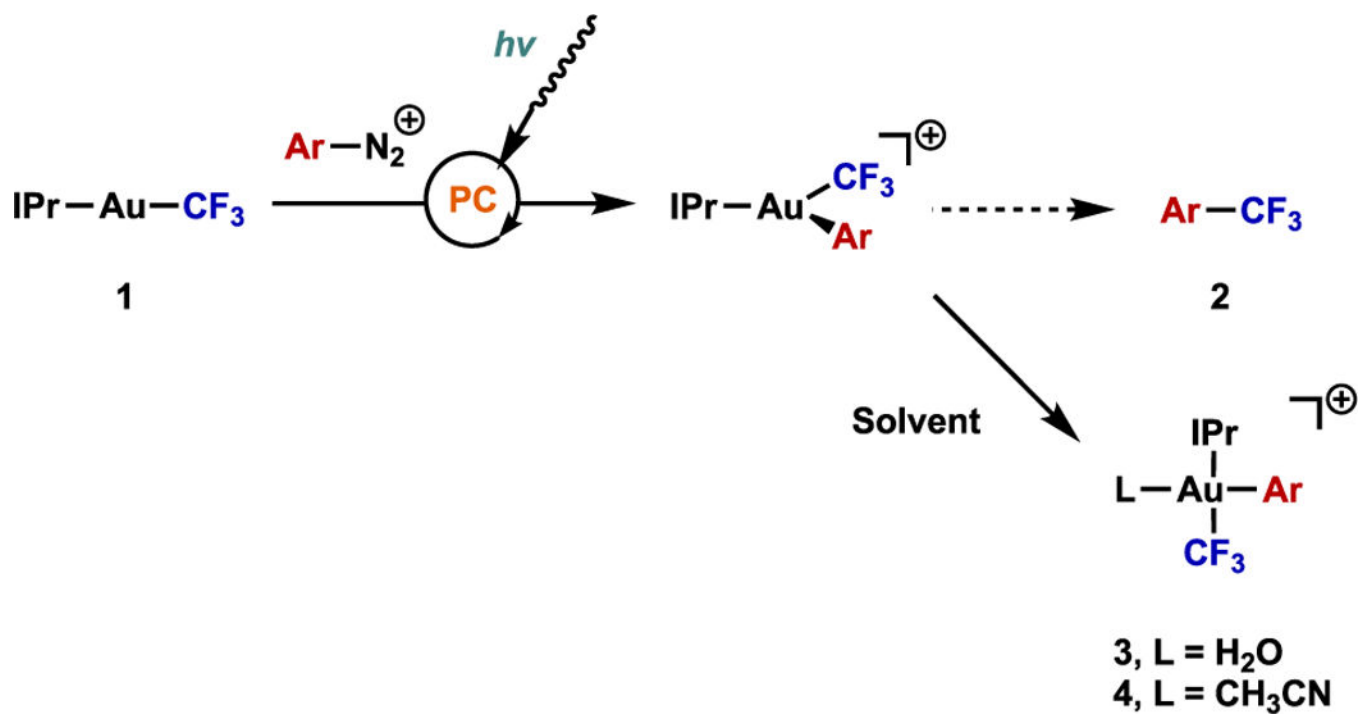(Bottom) UV–vis absorption spectra of all chemicals (concentration = 0.05 mM in
CH_3NO_2) and emission spectrum of the light source, Kessil H150.
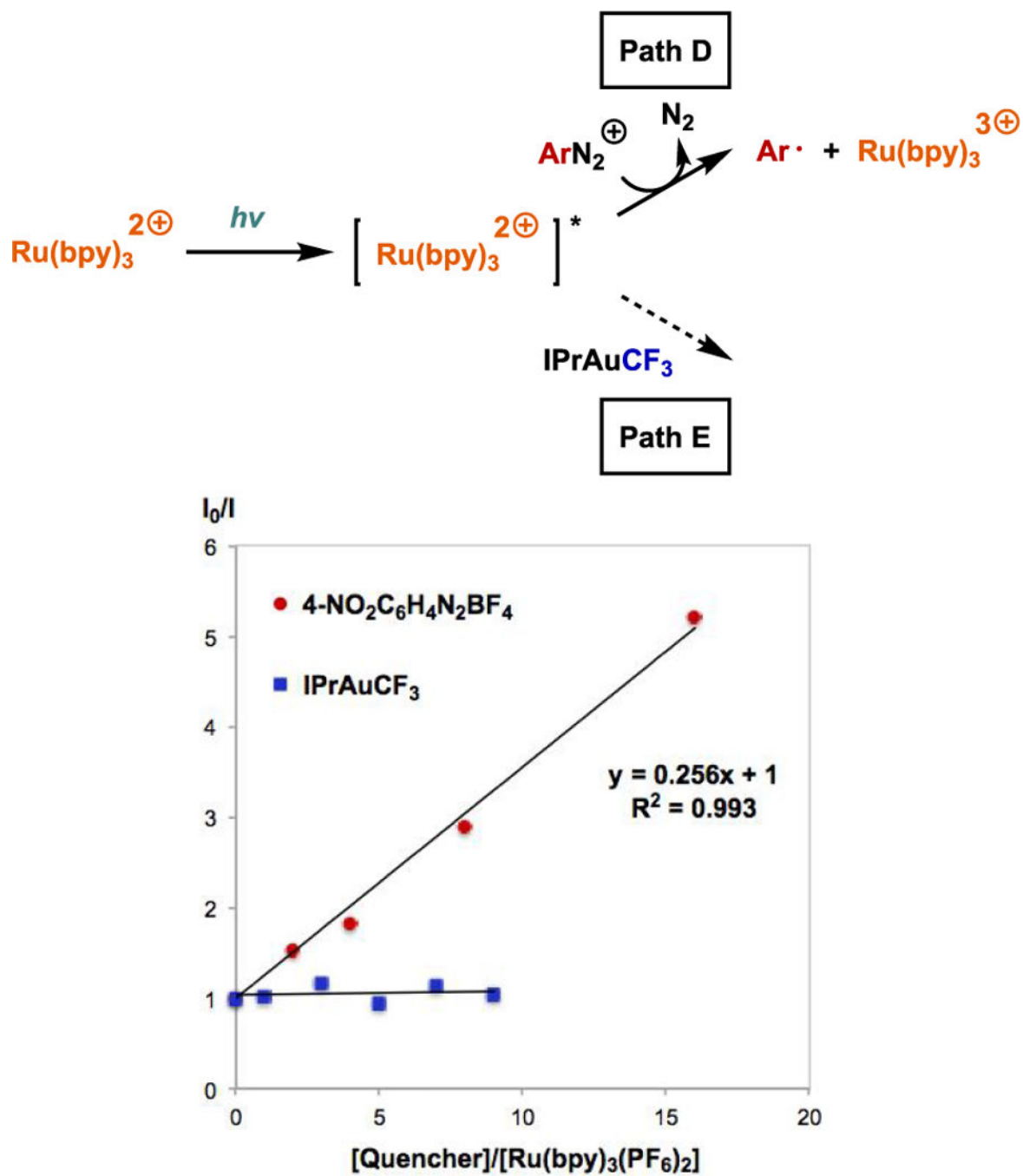
Figure 4.
(Top) Two possible modes of photoluminescence quenching. Path E was ruled out. (Bottom)
Stern–Volmer relationship. [Ru(bpy)$_3$(PF$_6$)$_2$] = 0.05 mM in CH$_3$NO$_2$.
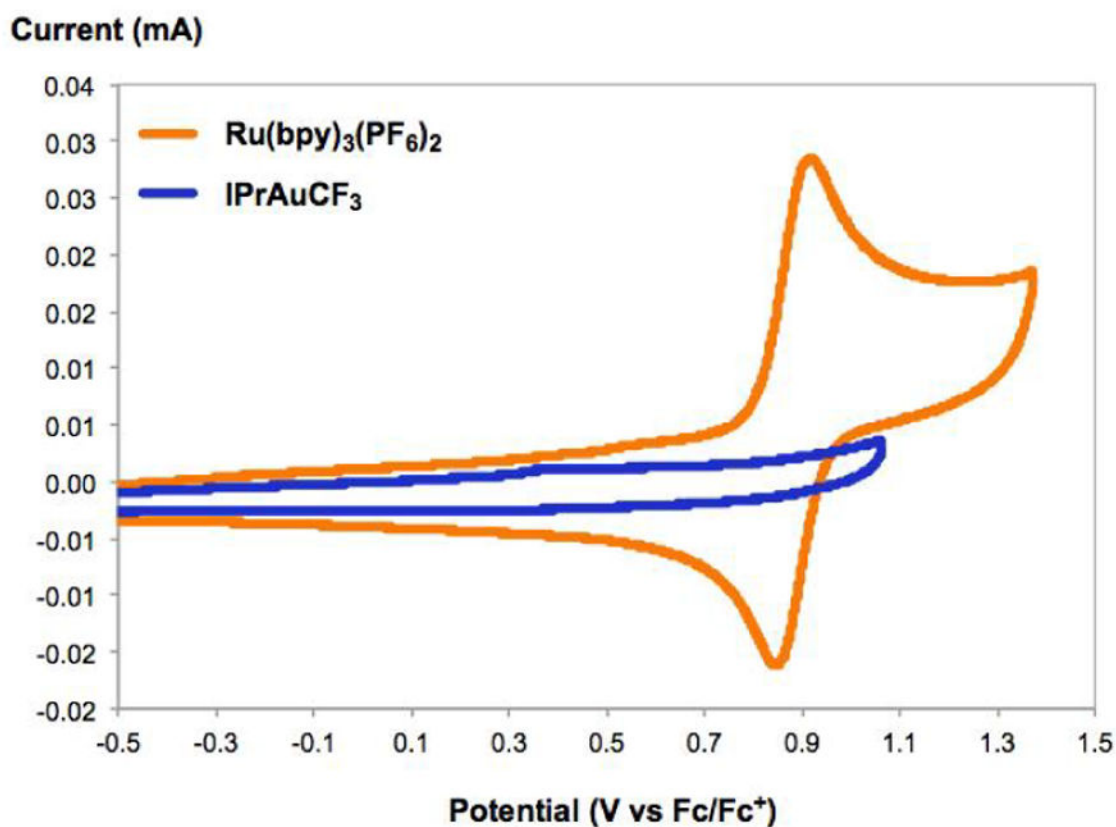
Figure 5.
(Top) Two possible reaction mechanisms of oxidative addition. (Bottom) Cyclic voltammogram of $Ru(bpy)_3(PF_6)_2$ and $IPrAuCF_3$, scan rate = 100 mV/s.
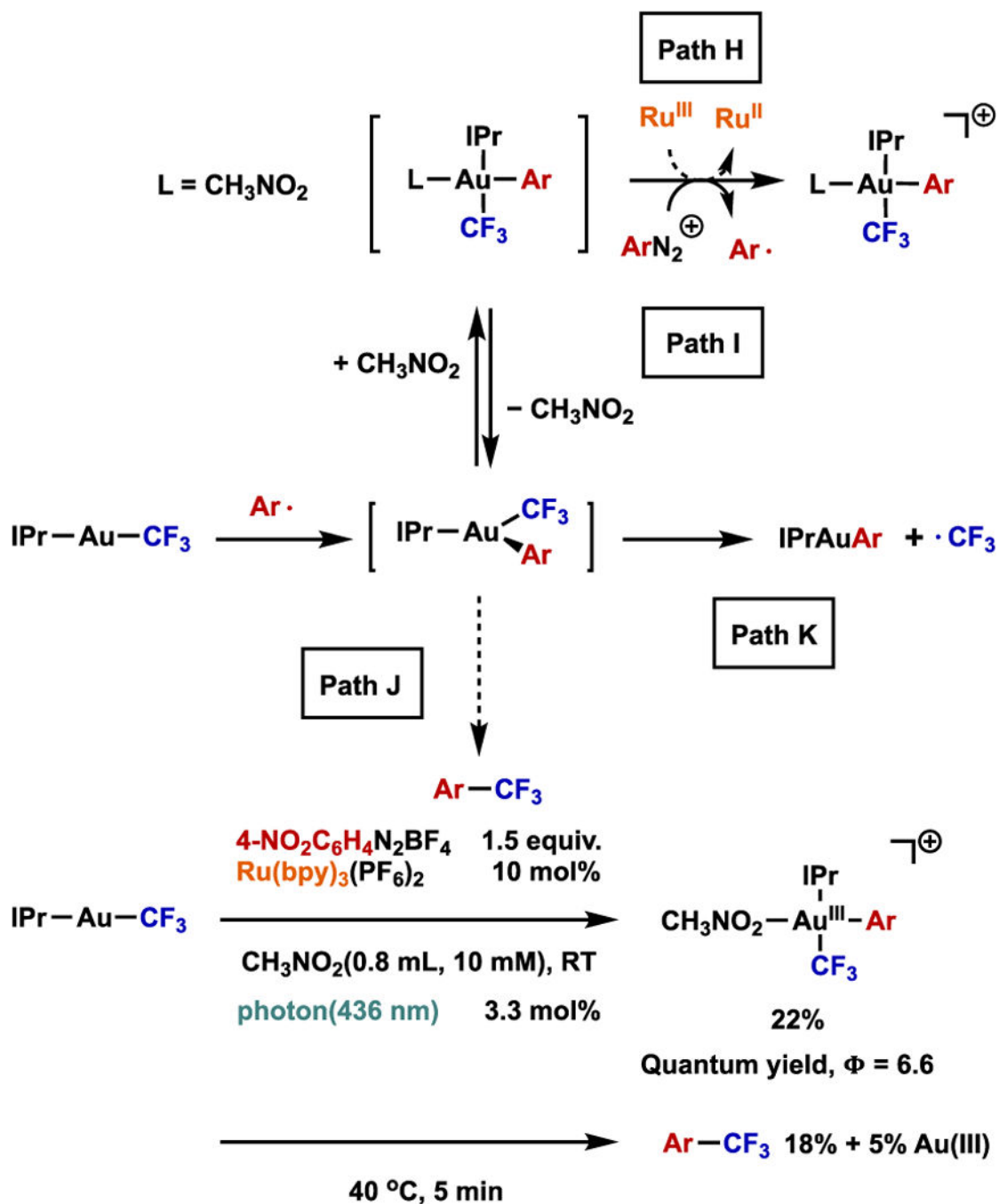
Figure 6.
(Top) Revised reaction mechanism of oxidative addition. The major operating pathway is path I. Path J was not observed. (Bottom) Quantum yield and reductive elimination of CH$_3$NO$_2$-bound gold(III) intermediate. Yields are reported in triplicate.
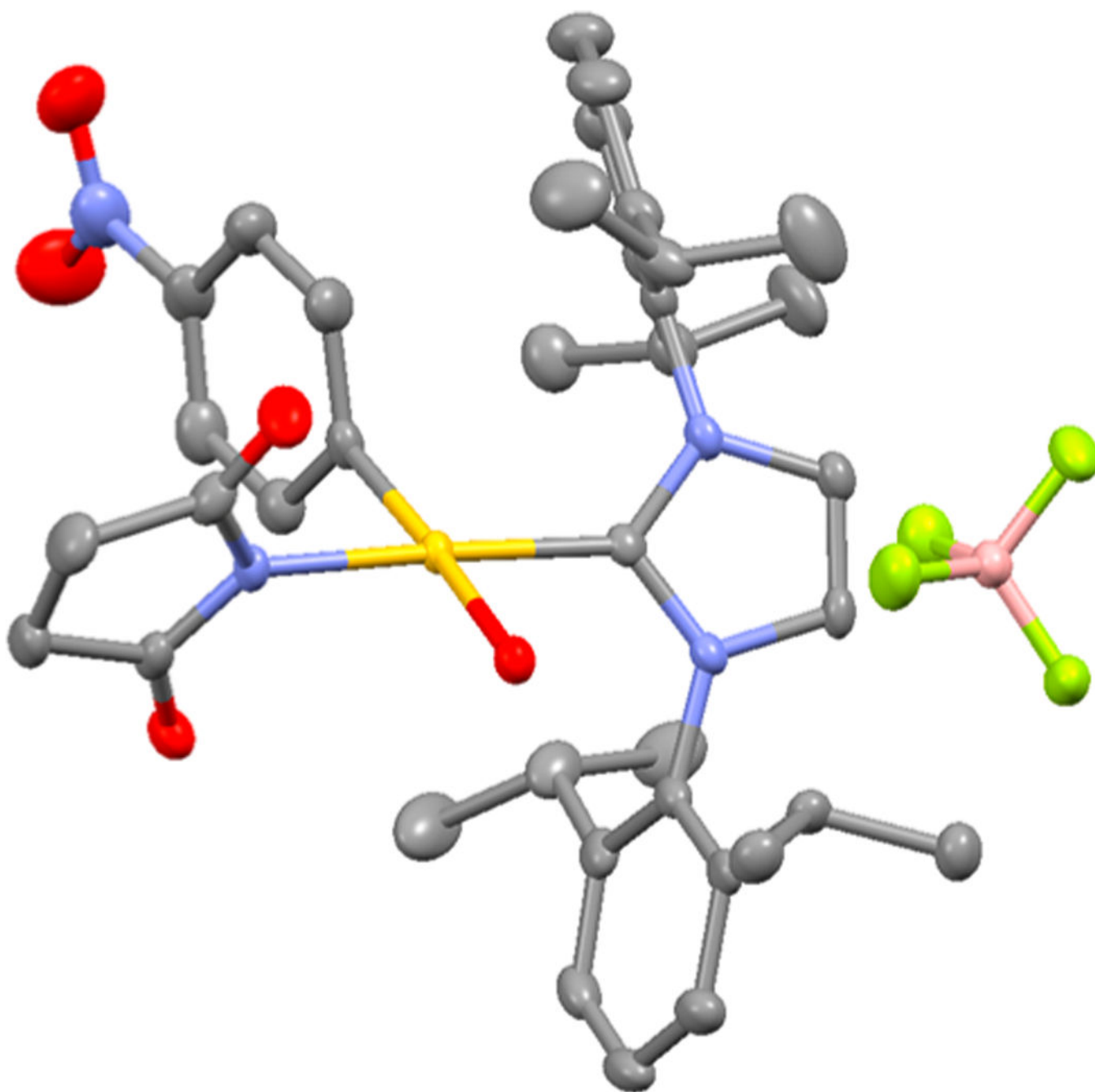
Figure 7.
Crystal structure of 7-BF$_4$. Thermal ellipsoid plot is drawn at 50% probability. Hydrogen
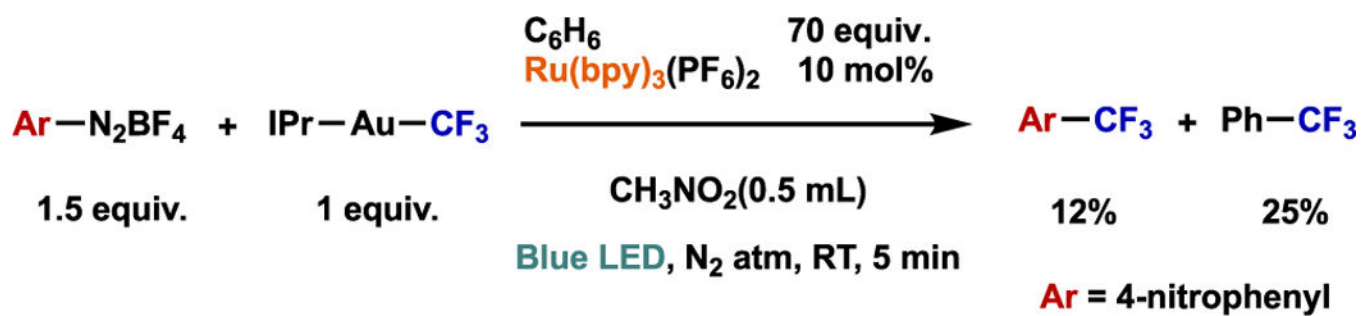atoms and solvents are omitted for clarity.
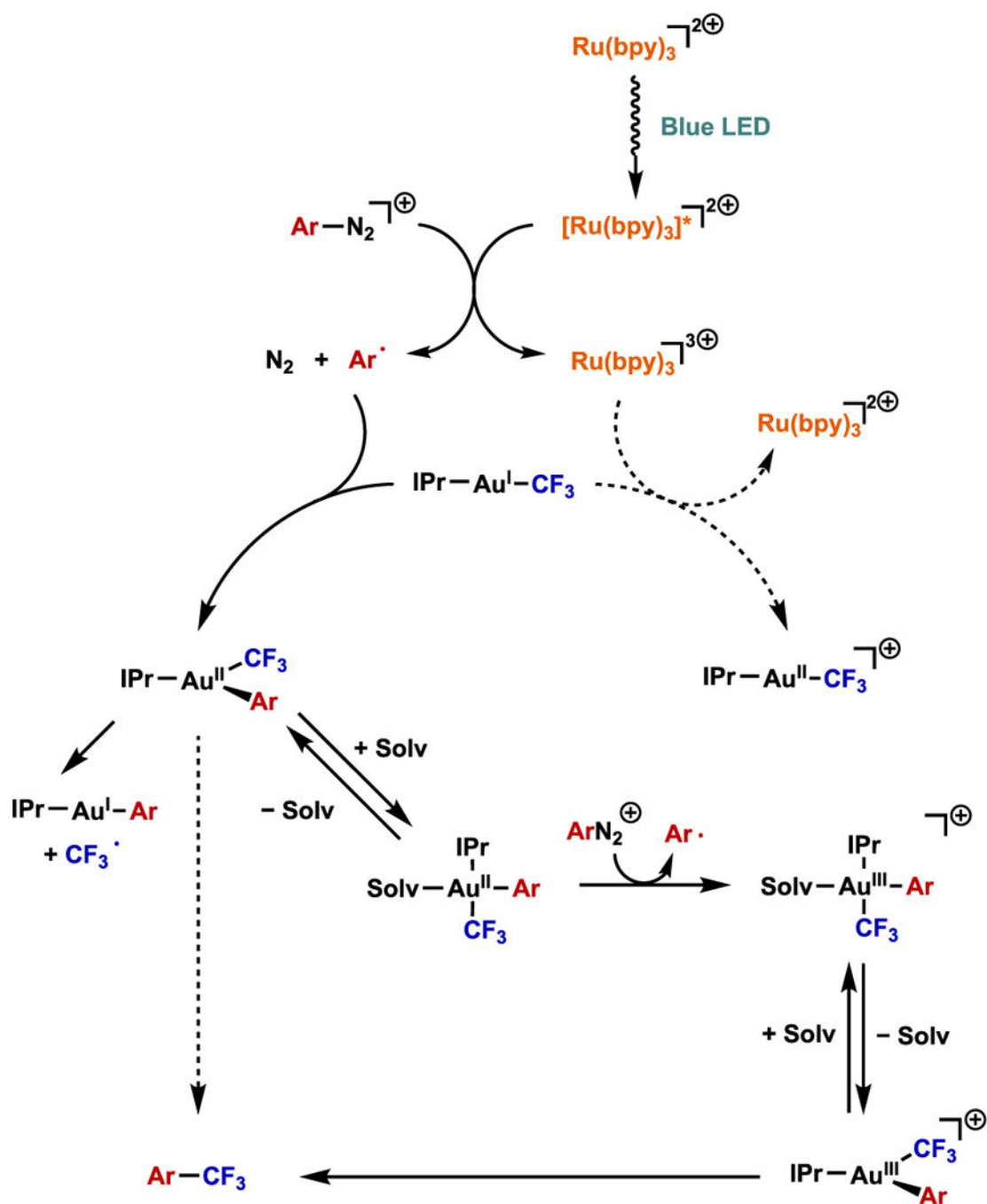
Figure 8.
Summary of proposed reaction mechanism, Solv = CH_3NO_2.
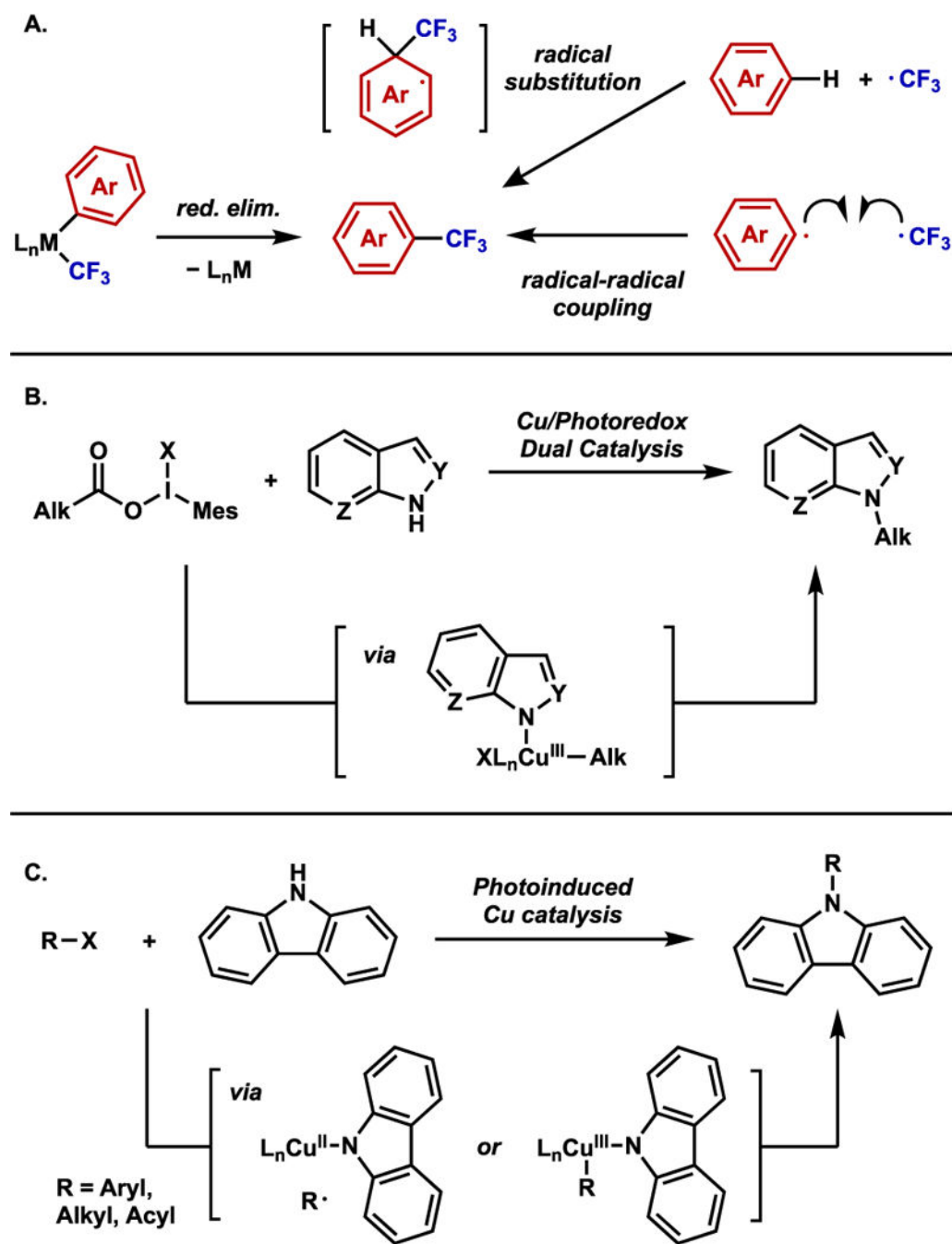
Scheme 1.
Potential Bond-Forming Steps of Metallaphotoredox Catalysis (A) Copper(III)
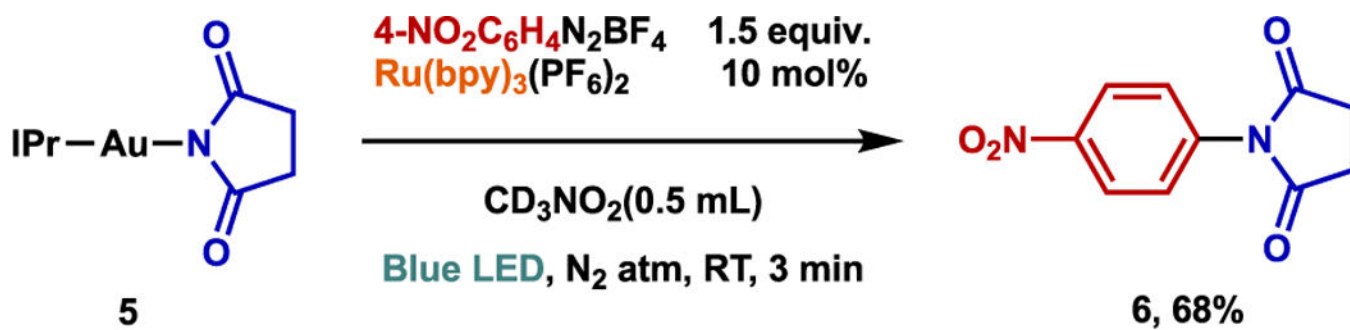Intermediates Proposed for Photochemical C–N Coupling Reactions (B and C)

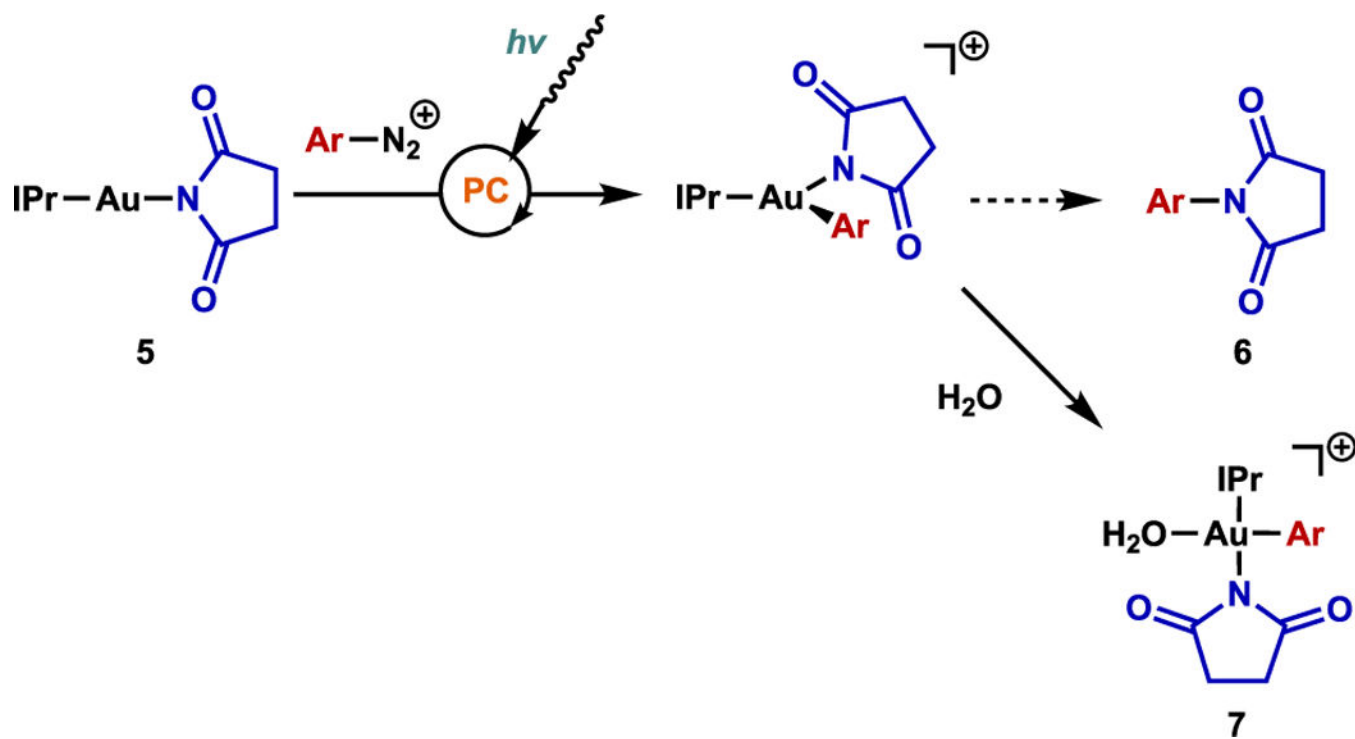**Scheme 2.**
Intercepted Gold(III)−CF$_3$ Intermediates[a]

$$Ar-N_2BF_4 \quad + \quad IPr-Au-CF_3 \quad \xrightarrow[\substack{CH_3NO_2(0.5 \text{ mL}) \\ \textbf{Blue LED, N}_2 \text{ atm, RT, 5 min}}]{\substack{C_6H_6 \quad 70 \text{ equiv.} \\ Ru(bpy)_3(PF_6)_2 \quad 10 \text{ mol\%}}} \quad Ar-CF_3 \quad + \quad Ph-CF_3$$

1.5 equiv.   1 equiv.   12%   25%

Ar = 4-nitrophenyl
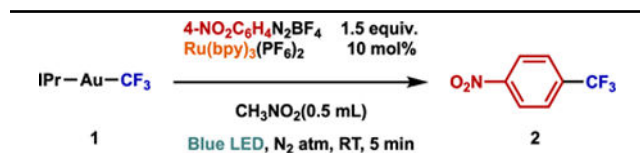
Scheme 3.
Radical Trapping Experiment

Scheme 4.
Photoredox-Initiated Gold-Mediated C(sp^2)–Succinimide Coupling Reaction[a]

Scheme 5.
Intercepted Gold(III)−Succinimide Intermediate[a]

Table 1.

Control Experiment[a,b]

| entry	variation from the reaction condition	yield[c,d]
1	none	60%
2	no catalyst	<1%
3	dark and 40 °C instead of blue LED and rt	<1%
4	ArI(Mes)OTf instead of ArN_2BF_4	22%
5	$Ir(ppy)_2(dtbbpy)PF_6$ instead of $Ru(bpy)_3(PF_6)_2$	11%
6	$Ir\{dF(CF_3)ppy\}_2(dtbbpy)PF_6$ instead of $Ru(bpy)_3(PF_6)_2$	18%
7	$Ru(bpz)_3(PF_6)_2$ instead of $Ru(bpy)_3(PF_6)_2$	19%
8	$Cu(dap)_2Cl$ instead of $Ru(bpy)_3(PF_6)_2$	<1%
9	$Mes-AcrBF_4$ instead of $Ru(bpy)_3(PF_6)_2$	7%
10	under air instead of three freeze–pump–thaw cycles	24%
11	$CH_3NO_2:H_2O = 96:4$ (v/v) instead of CH_3NO_2	<1%[e]

[a]Reactions run at 8 μmol scale.

[b]The temperature increases up to 40°C.

[c]19F NMR yield by using $PhOCF_3$ as an internal standard.

[d]In triplicate.

[e]9% of $IPrAuCF_3$ and 55% of $Au^{III}CF_3$ were observed.

Table 2.

Electronic Effect on Aryldiazonium[a,b]
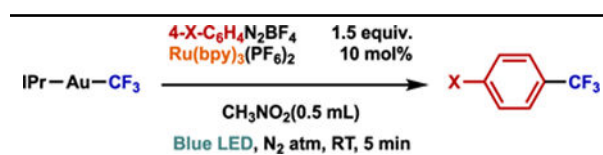
entry	X	yield[c,d]
1	NO_2	60%
2	CO_2Me	48%
3	Ac	43%
4	Br	46%
5	Cl	52%
6	F	44%
7	H	19%
8	Me	17%
9	*tert*-Bu	16%
10	OMe	15%

[a] Reactions run at 8 μmol scale.

[b] The temperature increases up to 40 °C.

[c] 19F NMR yield by using PhOCF3 as an internal standard.

[d] In triplicate.